LETTER

doi:10.1038/nature10749

Origin of Columbia River flood basalt controlled by propagating rupture of the Farallon slab

Lijun Liu[1] & Dave R. Stegman[1]

The origin of the Steens–Columbia River (SCR) flood basalts, which is presumed to be the onset of Yellowstone volcanism, has remained controversial, with the proposed conceptual models involving either a mantle plume[1–5] or back-arc processes[6–8]. Recent tomographic inversions based on the USArray data reveal unprecedented detail of upper-mantle structures of the western USA[9] and tightly constrain geodynamic models simulating Farallon subduction, which has been proposed to influence the Yellowstone volcanism[5,6]. Here we show that the best-fitting geodynamic model[10] depicts an episode of slab tearing about 17 million years ago under eastern Oregon, where an associated sub-slab asthenospheric upwelling thermally erodes the Farallon slab, leading to formation of a slab gap at shallow depth. Driven by a gradient of dynamic pressure, the tear ruptured quickly north and south and within about two million years covering a distance of around 900 kilometres along all of eastern Oregon and northern Nevada. This tear would be consistent with the occurrence of major volcanic dikes during the SCR–Northern Nevada Rift flood basalt event both in space and time. The model predicts a petrogenetic sequence for the flood basalt with sources of melt starting from the base of the slab, at first remelting oceanic lithosphere and then evolving upwards, ending with remelting of oceanic crust. Such a progression helps to reconcile the existing controversies on the interpretation of SCR geochemistry and the involvement of the putative Yellowstone plume. Our study suggests a new mechanism for the formation of large igneous provinces.

The SCR igneous province of the Pacific Northwest represents one of the largest continental flood basalt events, with a total eruption volume of around 230,000 km^3 over approximately two million years (Myr) (ref. 3). This massive, fast eruption seems to favour a mantle plume origin[1–3], but a plume model cannot address why most SCR flood basalt erupted in a north–south-oriented region perpendicular to the subsequent Yellowstone hotspot track along the eastern Snake River plain (Fig. 1). Recent models trying to explain this complexity include spreading of the plume head along a lithospheric gradient[4] and lateral deflection of the plume conduit due to mantle flow[5]. Other workers, however, dismissed the plume hypothesis as conjecture, and argued that the SCR event could have been a result of shallow-mantle processes, such as back-arc extension[6] or small-scale convection[7] or lithosphere delamination[8]. These conceptual models are all based on some aspects of surface geologic features, but the implied underlying mantle dynamics differ significantly from each other. A better understanding of the SCR flood basalt formation, therefore, requires an improved knowledge of mantle processes during the mid-Miocene epoch (about 16 Myr ago), especially given that Farallon subduction adequately explains both the observed surface plate kinematics and continental deformation within the western United States.

A promising way to infer past mantle dynamics is by predicting its present-day state through geodynamic modelling using a technique called data assimilation, which can be either sequential[11] or variational[12]. Here we adopt the sequential technique and assimilate plate motion history, palaeo-seafloor ages and palaeo-geometry of plate boundaries into a single geodynamic model[10]. The model integrates from 40 Myr ago to the present, through which we try to predict the observed mantle structures beneath the western USA outlined with increasing detail by a sequence of tomographic inversions based on data from the USArray[9] (see Supplementary Fig. 1 for more tomography models). The most robust seismic feature, a 500-km-wide columnar fast anomaly extending from 300 to 600 km depth below Nevada and western Utah, was found to be a segmented piece of the Farallon slab that was folded upward along its edges by toroidal mantle flows during its descent (Supplementary Fig. 2). Tracking backward in time, the initial break-off of this slab happened around 17 Myr ago at shallow depth (Figs 1 and 2). This is because the shrinking width of the

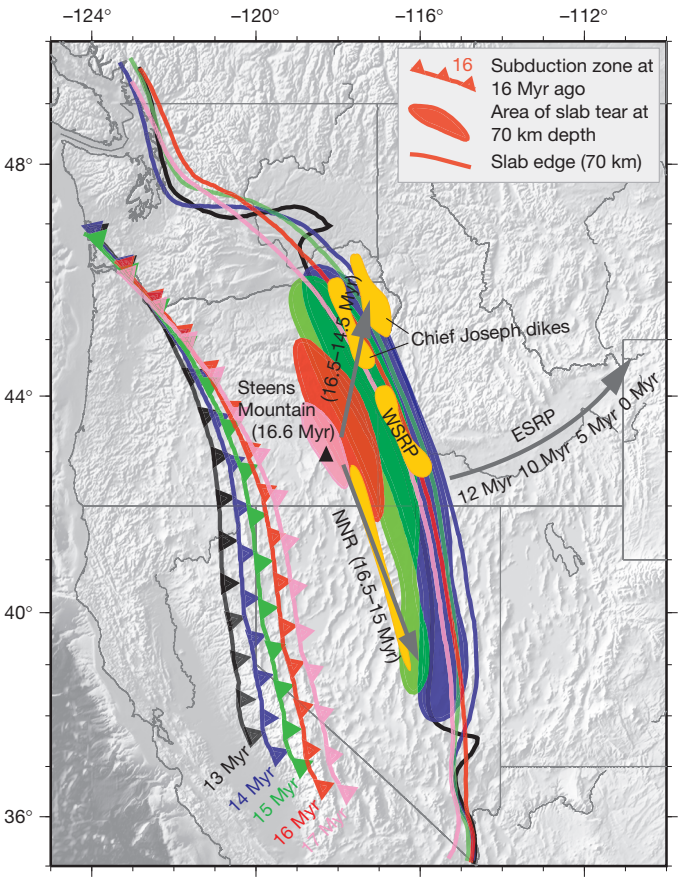

Figure 1 | Development of the Farallon slab rupture beneath the western USA during the mid-Miocene epoch. Geometry of Farallon subduction at different times (corresponding to different colours, ages in Myr as shown) is projected onto North America. Both the slab edge (solid lines) and slab gap (filled area) are at 70 km depth, outlined by an isotherm (−50 °C relative to ambient mantle). Major SCR volcanic dikes following ref. 27 are shown as yellow patterns (with ages in Myr shown). Grey arrows indicate the direction of age (shown, in Myr) progression of surface eruptions. WSRP, western Snake River plain; ESRP, eastern Snake River plain; NNR, northern Nevada rift zone.

[1]IGPP, Scripps Institution of Oceanography, University of California, San Diego, La Jolla, California 92093, USA.

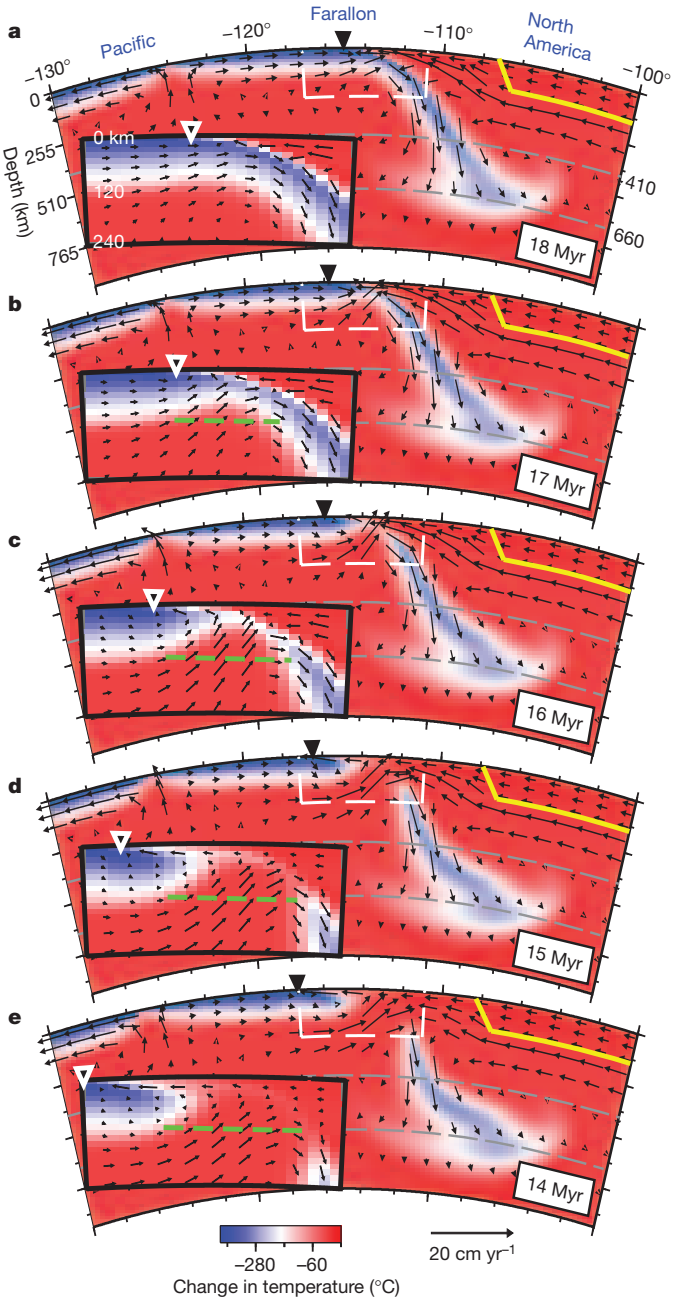

Figure 2 | Mantle flow associated with the slab tearing at latitude 44 °N from 18 to 14 Myr ago. Axes in **b**–**e** are the same as those in **a**. Solid yellow outlines represent the high-viscosity North America continent. Inverse black triangles mark trench locations with time. Insets are zoom-in plots of the subduction zones outlined by the white dashed boxes. The green dashed line represents the depth of 110 km, above which melting would occur[18]. We do not explicitly model melt generation because parameterizations of melting processes commonly implemented are applicable to melting of ambient mantle material and are not relevant to different compositions such as oceanic lithosphere and oceanic crust, as in the scenario presented here. Black arrows show mantle velocities, and the change in temperature is relative to the ambient mantle.

oceanic plate[13] gradually built up dynamic pressure beneath the middle part of the subducting slab, where the increased pressure caused the slab to flatten[10] (see Fig. 2a for example). Consequently, the flattening slab slowed down the forward plate motion, and sped up back-arc extension, as predicted by fully dynamic subduction models[14]. The reduction in plate motion and regionally focused sub-slab dynamic pressure generated an extension in the central part of the slab hinge, which, combined with thermal erosion due to sub-slab upwelling, caused the weak slab to stretch and eventually break in the middle[10] (Figs 2 and 3), similar in some ways to slab tear migrations proposed for Mediterranean slabs[15].

To understand the possible surface effects of this slab tear, we project the Farallon subduction system onto the reference frame of North America, neglecting the internal deformation of the western USA due to Basin and Range extension[16]. The initial slab tear occurred as early as about 17 Myr ago, which, in a map view, formed a trench-parallel slab gap (defined by an isotherm at a depth of 70 km) inside the back-arc region beneath southeastern Oregon (Fig. 1). This gap coincides with the location of Steens Mountain, which recorded the initial phase of eruption during the SCR flood basalt event. The slab tear ruptured quickly to north and south along the trench-parallel direction (Fig. 3), while at the same time the progressive flattening shifted the slab gap to the east (Figs 1 and 2). By 15 Myr ago, the gap occupied all of east Oregon, southwest Idaho and north Nevada (Fig. 1). This propagating pattern of slab tear correlates with the sequence of major mid-Miocene volcanic dikes both in space and time. From south to north with decreasing age, the western Snake River plain and Chief Joseph dike swarms hosted an increasing amount of magma outpouring, forming the Imnaha and Grande Ronde magmatic provinces[4], consistent with the northward rupturing and widening of the slab gap. Meanwhile, the southward slab rupturing with a narrower gap also explains the rapid formation (within about 1.5 Myr) of the northern Nevada rift zone[27] and the observed limited magma eruption along this region. Furthermore, the reduction of trenchward wedge flow inside Oregon after 17 Myr ago (Figs 2 and 3) provides a physical explanation for the reduced magmatic activities along the Oregon coastal arc since this time[17]. About 14 Myr ago, the Farallon slab was largely separated into two pieces along the down-dip direction, the landward extent of flat slab underplating started to retreat to the west (Figs 1 and 2), and sub-slab pressure was largely equilibrated with the mantle wedge, consistent with termination of the SCR eruption around this time[4].

Another important condition for making flood basalts is sufficient subsurface mantle upwelling, which is a salient feature of the mantle plume model. We also observe a strong focused mantle upwelling below the slab hinge, driven by the excess dynamic pressure beneath the subducting plate (Figs 2 and 3). Melting in this setting can reasonably be expected, because melts are generated at depths shallower than 110 km along forced upwellings in oceanic environments[18]. This fast upwelling flow advectively erodes the slab isotherm, leading to a progressively shallower asthenosphere, which suggests that oceanic lithosphere would melt first, followed by melting of oceanic crust. The modelled slab initially acted as both a thermal and mechanical barrier to upward flow and inhibited melting, as can be seen from 18 Myr ago, when the upwelling simply flattened the slab (Fig. 2a, inset). Subsequent thermal erosion of the oceanic lithosphere (Fig. 2b) would allow melt production under the Steens Mountain and Imnaha provinces (Table 1). By 16 Myr ago, continued thermal erosion melted away the entire oceanic lithosphere (Fig. 2c), where the fast melting of oceanic crust encountering the high mantle temperature should have triggered the massive magma outpouring of Grande Ronde[4]. The sustained cooling within the upwelling due to progressive melting seems to explain the marked decrease in magma volume during the formation of the Imnaha province (Table 1) and the step-function change in chemistry at the Imnaha–Grande Ronde boundary[19]. The upward corner flow inside the mantle wedge may also have facilitated melt generation, but its volume contribution is probably minor, given the much colder environment below the overriding plate, an aspect not explicitly represented in our convection model (Figs 2 and 3).

The geochemical data, essential for determining the source rocks, have been used both for and against a plume signature in the SCR lavas[1,3,19–21]. Although origins of both major and trace elements are still widely debated among existing conceptual models, there are certain points of consensus (Table 1). (1) Steens Mountain lavas are derived from an ultra-depleted mantle source[20], probably "owing to repetitive

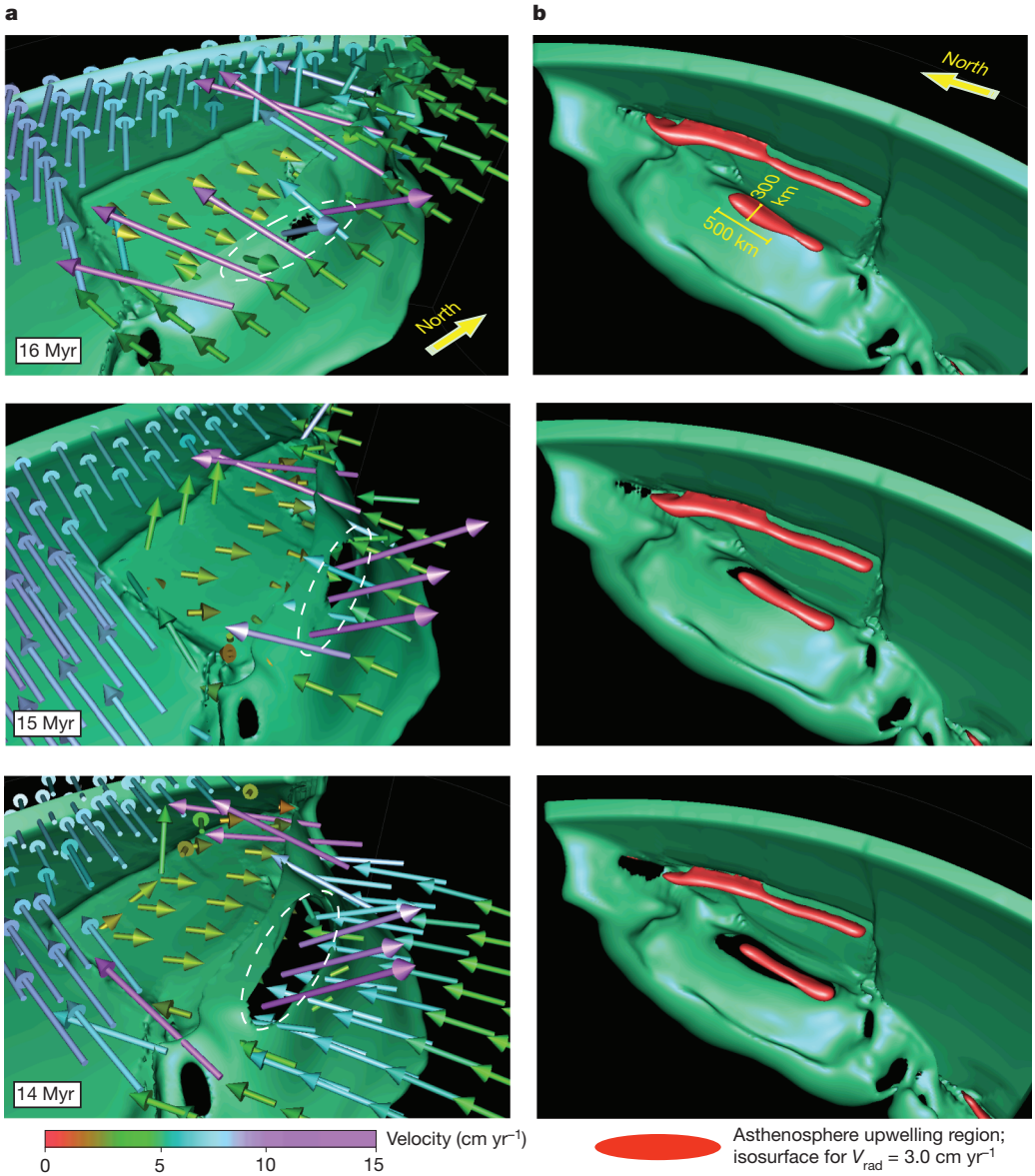

Figure 3 | Three-dimensional view of the tearing slab. **a**, Top view of an isothermal slab surface (−100 °C relative to ambient temperature) and the velocity field. The velocity vectors are on the same spherical plane across all surface plates. The white dashed oval outlines a region where asthenosphere upwelling occurred. We note that the upwellings are restricted to below the Farallon slab where velocity vectors originate (see Fig. 2 for detailed flow fields). **b**, Bottom view showing distribution of asthenosphere upwellings beneath the mid-ocean ridge (long red shape) and propagating slab tear (short red shape). The region inside the red surface represents mantle upwelling with radial velocity magnitudes >3 cm yr^{-1}.

extraction of trace-element magmas"[1]. (2) The Grande Ronde lavas have the highest silica content of all SCR lavas[19], and are best explained by melting of a mafic crust[22]. (3) The SCR formations experienced a progressive assimilation of material from the overriding continent and from subducted sediments[1,19,20].

These three features are consistent with our proposed bottom-up melting model as follows. The earliest eruption at Steens Mountain is derived from the depleted subducting oceanic lithosphere, whose melts also tend to be low in silica content. The upward melting across the subducting slab will eventually melt its mafic crust in an avalanche

Table 1 | Summary of SCR basalts and proposed mechanisms

SCR formation[4]	Geochemical property[1,19–21]	Volume[3,4] (km^3)	Source composition	Unreconciled aspects of previous models
Steens (16.6–16.2 Myr)	Low silica content; high ε_{Nd}, low $^{87}Sr/^{86}Sr$, incompatible element depletion	60,000	Subducting oceanic lithosphere	Highly depleted magma source (plume-head models[1–5], lithosphere-plume[19] or slab–plume[25] interactions)
Imnaha (16.3–16.1 Myr)	Excess $^{206,208}Pb/^{204}Pb$, excess Th, Nb and $^3He/^4He$	10,000	Subducting oceanic lithosphere and sediments or mantle plume	
Grande Ronde (16.1–15.0 Myr)	Silica saturated; low ε_{Nd}, high $^{87}Sr/^{86}Sr$, chemically homogeneous, incompatible element enrichment	150,000	Subducting oceanic crust and sediments and Archean mantle lithosphere	High SiO_2 and homogeneity (plume-head models[1–5], lithosphere-plume[19] or slab–plume[25] interactions) and large volume and high SiO_2 (back-arc processes[6–8])

fashion, which best explains Grande Ronde's homogeneous composition, saturation in silica content, and high-degree of incompatible elements enrichment[20]. With the mantle isotherm shifted towards shallower depths, a progressive involvement of sediments from the subducted sea floor and of the overriding lithosphere and crust is expected, which explains the transitional composition of Imnaha lavas[19,20]. Our proposed mechanism, however, does not preclude the existence of secondary crustal processes, such as crystal fractionation, before surface eruption.

Of all SCR formations, elevated $^3He/^4He$ ratios in a subpopulation of Imnaha basalts are the only ones that might indicate a mantle plume signature[21]. However, involvement of a plume head should lead to both highly heterogeneous and enriched compositions throughout SCR lavas, which is contrary to observations and suggests that if a mantle plume ever existed, it played a very minor part in defining the SCR flood basalt. The remarkable spatial/temporal correlations shown in Fig. 1 and the consistency with geochemistry (Table 1) strongly favour a slab-rupture model over those with a plume-head origin. Furthermore, Palaeocene–Eocene-aged coastal ranges are interpreted as an accreted island chain formed by the Yellowstone hotspot[23,24] and provide possible evidence for a long-lived Yellowstone plume conduit that pre-dates the SCR event. We speculate that the Farallon slab captured the plume conduit and caused a short hiatus of Yellowstone-related volcanism during the early Miocene epoch, consistent with the plume-affinity of Imnaha basalts resulting from a northeast-deflected plume conduit[25]. Subsequently, accompanying the slab rupture, the plume conduit was reestablished to its original position along the ESRP[2,4], where a slab gap has existed throughout the upper mantle till the present day[10], and provided a path for the plume conduit to reach the surface (Supplementary Fig. 2). However, the interactions of this putative plume conduit with the Farallon slabs remain to be clarified.

METHODS SUMMARY

To explain the complex present-day mantle structure beneath the western USA, we use forward geodynamic models to simulate Farallon subduction during the past 40 Myr (ref. 10). The models are consistent with several types of palaeo-records, where both the initial and boundary conditions are observationally constrained. The thermal structure of the oceanic plate is according to palaeo-sea floor ages. With a high numerical resolution of down to 7 km, the models can effectively represent sophisticated thermal and rheological structures along plate boundaries, including mid-ocean ridges, transform faults, and subduction zones. The viscosity profiles of these fine features, especially those along convergent plate boundaries, are constrained such that the subducting slab hinge closely follows the time history of observed trench locations. We also introduce a pseudo free-surface function such that subduction occurs more naturally than in models without this function.

The Mid-Miocene slab tear event as described in this paper was critical for the formation of the present-day mantle structure. We find that although the exact shape and position of present mantle structure are very sensitive to the magnitude of mantle and slab viscosities[10], the slab tear starting at around 17 Myr ago was not: the tear always occurred with similar timing and location even when mantle viscosities varied by one order of magnitude around the best-fit values[10]. This slab tear, however, no longer occurred when we excluded the pseudo free-surface function in the calculation, indicating that the near-trench sub-slab dynamic pressure controls formation of the slab tear (Supplementary Fig. 3). Of all the models, the one that best predicts the seismic image also seems to match the SCR flood basalt stratigraphy best, which provides another validation for the geodynamic model.

Full Methods and any associated references are available in the online version of the paper at www.nature.com/nature.

Received 5 July; accepted 2 December 2011.

1. Brandon, A. D. & Goles, G. G. A Miocene subcontinental plume in the Pacific Northwest: geochemical evidence. *Earth Planet. Sci. Lett.* **88,** 273–283 (1988).
2. Pierce, K. L. & Morgan, L. A. in *Regional Geology of Eastern Idaho and Western Wyoming* (eds Link, P. K. *et al.*) **179,** 1–53 (Geological Society of America Memoir, 1992).
3. Hooper, P. R., Camp, V. E., Reidel, S. P. & Ross, M. E. The origin of the Columbia River flood basalt province: plume versus nonplume models. *GSA Spec. Pap.* **430,** 635–668 (2007).
4. Camp, V. E. & Ross, M. E. Mantle dynamics and genesis of mafic magmatism in the intermontane Pacific Northwest. *J. Geophys. Res.* **109,** B08204 (2004).
5. Smith, R. B. *et al.* Geodynamics of the Yellowstone hotspot and mantle plume: seismic and GPS imaging, kinematics, and mantle flow. *J. Volcanol. Geotherm. Res.* **188,** 26–56 (2009).
6. Carlson, R. W. & Hart, W. K. Crustal genesis on the Oregon plateau. *J. Geophys. Res.* **92,** 6191–6206 (1987).
7. Christiansen, R. L., Foulger, G. R. & Evans, J. R. Upper mantle origin of the Yellowstone hot spot. *Geol. Soc. Am. Bull.* **114,** 1245–1256 (2002).
8. Hales, T. C., Abt, D. L., Humphreys, E. D. & Roering, J. J. Delamination origin for the Columbia River flood basalts and Wallowa Mountain uplift in NE Oregon, USA. *Nature* **438,** 842–845 (2005).
9. Sigloch, K. Mantle provinces under North America from multifrequency P wave tomography. *Geochem. Geophys. Geosyst.* **12,** Q02W08 (2011).
10. Liu, L. & Stegman, D. R. Segmentation of the Farallon slab. *Earth Planet. Sci. Lett.* **311,** 1–10 (2011).
11. Bunge, H.-P. & Grand, S. P. Mesozoic plate-motion history below the northeast Pacific Ocean from seismic images of the subducted Farallon slab. *Nature* **405,** 337–340 (2000).
12. Liu, L., Spasojević, S. & Gurnis, M. Reconstructing Farallon plate subduction beneath North America back to the Late Cretaceous. *Science* **322,** 934–938 (2008).
13. Atwater, T. & Stock, J. in *Integrated Earth and Environmental Evolution of the Southwestern United States* (eds Ernst, W. G. & Nelson, C. A.) 393–420 (Bellwether Publishing, 1998).
14. Schellart, W. P., Stegman, D. R., Farrington, R. J., Freeman, J. & Moresi, L. Cenozoic tectonics of western North America controlled by evolving width of Farallon slab. *Science* **329,** 316–319 (2010).
15. Wortel, M. J. R. & Spakman, W. Subduction and slab detachment in the Mediterranean–Carpathian region. *Science* **290,** 1910–1917 (2000).
16. McQuarrie, N. & Wernicke, B. An animated tectonic reconstruction of southwestern North America since 36 Ma. *Geosphere* **1,** 147–172 (2005).
17. Priest, G. R. Volcanic and tectonic evolution of the cascade volcanic arc, central Oregon. *J. Geophys. Res.* **95,** 19583–19599 (1990).
18. Hirth, G. & Kohlstedt, D. Water in the oceanic upper mantle: implications for rheology, melt extraction and the evolution of the lithosphere. *Earth Planet. Sci. Lett.* **144,** 93–108 (1996).
19. Camp, V. & Hanan, B. A plume-triggered delamination origin for the Columbia River basalt group. *Geosphere* **4,** 480–495 (2008).
20. Carlson, R. W. Isotopic constraints on Columbia River flood basalt genesis and the nature of the subcontinental mantle. *Geochim. Cosmochim. Acta* **48,** 2357–2372 (1984).
21. Dodson, A., Kennedy, B. M. & DePaolo, D. J. Helium and neon isotopes in the Imnaha Basalt, Columbia River basalt group: evidence for a Yellowstone plume source. *Earth Planet. Sci. Lett.* **150,** 443–451 (1997).
22. Takahahshi, E., Nakajima, K. & Wright, T. L. Origin of the Columbia River basalts: melting model of a heterogeneous mantle plume head. *Earth Planet. Sci. Lett.* **162,** 63–80 (1998).
23. Duncan, R. A. A captured island chain in the coast range of Oregon and Washington. *J. Geophys. Res.* **87,** 10827–10837 (1982).
24. Beck, M. E. Has the Washington-Oregon coast range moved northward? *Geology* **12,** 737–740 (1984).
25. Geist, D. & Richards, M. Origin of the Columbia Plateau and Snake River plain: deflection of the Yellowstone plume. *Geology* **21,** 789–792 (1993).
26. Humphreys, E. D., Dueker, K. G., Schutt, D. L. & Smith R. B.. Beneath Yellowstone: evaluating plume and nonplume models using teleseismic images of the upper mantle. *GSA Today* **10,** 1–6 (2000).
27. Glen, J. & Ponce, D. Large-scale fractures related to inception of the Yellowstone hotspot. *Geology* **30,** 647–650 (2002).

Supplementary Information is linked to the online version of the paper at www.nature.com/nature.

Acknowledgements We thank R. Carlson and D. Blackman for discussions. Computational resources were provided by XSEDE project EAR100021. L.L. was funded by the John Miles Fellowship and the Cecil and Ida Green Foundation. D.R.S. was supported in part by the G. Unger Vetlesen Foundation.

Author Contributions L.L. designed and performed the numerical models. Both authors contributed equally to idea development and result interpretation.

Author Information Reprints and permissions information is available at www.nature.com/reprints. The authors declare no competing financial interests. Readers are welcome to comment on the online version of this article at www.nature.com/nature. Correspondence and requests for materials should be addressed to L.L. (lil019@ucsd.edu).

METHODS

Model set-up. We used the three-dimensional spherical finite element code for mantle convection, CitcomS[28], to simulate Farallon subduction. The code solves for an incompressible Newtonian fluid within a regional spherical mantle shell. We adopted a mesh with $257 \times 257 \times 65$ nodes in latitude $\times$ longitude $\times$ depth, covering a physical domain of $60^\circ \times 100^\circ \times 2{,}760$ km, respectively. The mesh had variable grid spacing in all three dimensions such that resolution increased towards the centre and the surface, with the finest mesh grid having a block size of 12 km $\times$ 20 km $\times$ 7 km beneath the western USA. We ensured that the model box was wide enough to avoid sidewall-induced artificial flows. In our case, the box had the nearest vertical boundary over 2,000 km away from any part of the western USA. We also tested the effect of box depth on mantle flow and found that as long as the depth is larger than 1,000 km, the resulting upper mantle structures become similar. So we chose a mantle depth of approximately 2,700 km.

Initial and boundary conditions. These are essential components of a data assimilation model. The initial condition is both observationally constrained and numerically tested. The starting time of 40 Myr is consistent with both Cascada volcanism history[29] and present-day seismic tomography[30]. Tests suggest that subduction starting from this initial time are more than enough to properly capture the Farallon evolution since the Miocene, which is the time of interest in this study. The boundary conditions including both the thermal structure and surface kinematics are based on a recent plate reconstruction[31]. We define the top thermal boundary layer in oceanic plates using time-dependent palaeo-seafloor ages, with the profile largely following a half-space cooling model. The plate motions are imposed as top velocity boundary conditions at every time step during the calculation.

Another important feature adopted in our calculation is a pseudo-free surface implemented as a 'sticky air' layer on top of a viscous fluid, which has been shown to be successful in obtaining realistic slab geometry in the vicinity of a subduction zone as found in laboratory experiments[32]. We converted this sticky-air function into a phase transformation within the uppermost two elements of the model such that oceanic plate within this layer gains some extra negative buoyancy, to mimic the lateral pressure gradient at a convergent boundary due to the low topography of the trench. This effectively mimics the zero-density 'sticky air' implementation because they both increase the lateral gradient of buoyancy that promotes the plate's tendency to sink asymmetrically at the subduction front.

Rheologic structures. We use both depth- and temperature-dependent viscosity. A four-layer viscosity structure is assumed, including lithosphere, asthenosphere, transition zone, and lower mantle. The viscosity magnitudes of these layers are subsequently constrained by predicting the present-day seismic tomography image[10]. Density changes due to the phase transformation across the 410-km and 660-km interfaces were also considered. Lateral variation of viscosity is achieved first from temperature dependence, assuming a Newtonian fluid. We did not use a nonlinear rheology because of existing controversies over the viscous strength of mantle and slabs. We circumvent this problem by searching for the effective viscosity of ambient mantle and slabs so that we can best predict the observed slab morphology at the present day across the entire upper mantle. Furthermore, the model also incorporated many sharp rheological features such as narrow plate boundaries (vertical at mid-ocean ridges and transform faults, and one-side dipping above down-going slabs), slab hinges (weak bending parts of the slab with a stronger core), a mantle wedge (a weak zone between the surface and the slab), and large rheological variations from the Basin and Range province to the cratonic North America. In effect, the model can achieve a viscosity contrast of up to four orders of magnitude within a 100-km distance. We find that the resulting strong three-dimensional viscosity variation is essential for the generation of asymmetric subduction and a physically reasonable subducting slab whose hinge closely follows the position of trenches as a function of time.

Mid-Miocene slab tear. With the model set-up as described above, we find that a segmented present-day mantle structure can easily be reached[10]. However, to predict the exact structures as observed by tomography[33], we have to find the appropriate viscosities for both the ambient mantle and slabs. Interestingly, we find that, besides the best-fitting model, those runs whose viscosities are several times larger or smaller than the best-fitting ones still have the Farallon slab break at a similar time and location, even though their predicted present-day structures are entirely off. This suggests that the slab tear was not sensitive to the large-scale viscosity structure. The detailed viscosity profile of the subduction zone and mantle wedge, on the other hand, plays a major part in the behaviour of the subducting slab, including its smoothness, curvature and trench retreat rate. For the slab hinge to follow trench position through time, a critical constraint from observations, the subduction zone has to be weak. However, we did not find evidence that this fine-scale rheology structure controls the slab tear formation.

Other parameters that may control the slab tear include surface plate motions and sub-slab dynamic pressure. We found that the imposed surface kinematics cannot generate the slab tear without enough sub-slab dynamic pressure (removing the sticky-air function decreases the dynamic pressure under the slab): when plate motions slowed down and trench rollback increased during the Miocene as observed, the slab would simply roll back faster but still follow the trench position without breaking internally around the mid-Miocene (Supplementary Fig. 3). The sub-slab dynamic pressure, however, is more important. Because the dynamic pressure is an intrinsic property of the three-dimensional slab geometry, it cannot be entirely separated out for a sensitivity test in a multi-parameter model like the one we have. But we can test its effect by turning on and off the sticky air function whose existence increases the sub-slab dynamic pressure by acknowledging the effect of trench topography. We found that without the sticky air, the slab would never break around the mid-Miocene even with the slow-down of surface plates, and the predicted present-day mantle structures would never match the tomography image. With the sticky air, the excess sub-slab dynamic pressure associated with the shrinking width of the Farallon plate builds up with time, and eventually breaks the slab midway along the trench where the pressure is the greatest (Fig. 3, Supplementary Fig. 3).

28. Zhong, S., Zuber, M. T., Moresi, L. N. & Gurnis, M. The role of temperature dependent viscosity and surface plates in spherical shell models of mantle convection. *J. Geophys. Res.* **105,** 11063–11082 (2000).
29. Humphreys, E. Post-Laramide removal of the Farallon slab, western United States. *Geology* **23,** 987–990 (1995).
30. Sigloch, K., McQuarrie, N. & Nolet, G. Two-stage subduction history under North Amercia inferred from multiple-frequency tomography. *Nature Geosci.* **1,** 458–462 (2008).
31. Müller, R. D., Sdrolias, M., Gaina, C. & Roest, W. R. Age, spreading rates and spreading asymmetry of the world's ocean crust. *Geochem. Geophys. Geosyst.* **9,** Q04006 (2008a).
32. Schmeling, H. *et al.* A benchmark comparison of spontaneous subduction models—towards a free surface. *Phys. Earth Planet. Inter.* **171,** 198–223 (2008).
33. Schmandt, B. & Humphreys, E. Complex subduction and small-scale convection revealed by body-wave tomography of the western United States upper mantle. *Earth Planet. Sci. Lett.* **297,** 435–445 (2010).

doi:10.1038/nature10749

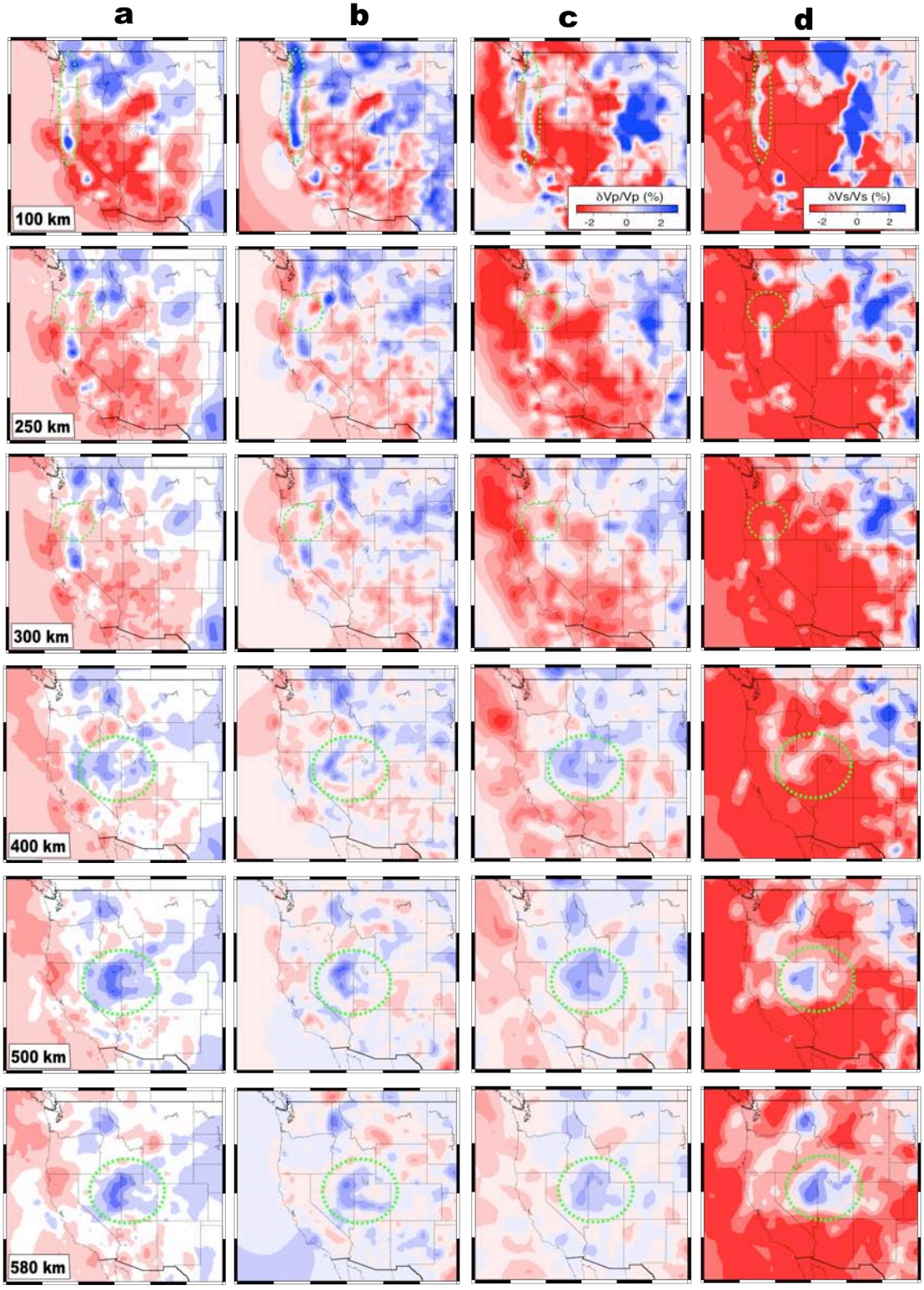

Figure S1. Tomographic images of western US upper mantle, from four recent studies based on the USArray seismic data. (**a-c**) Three P-wave models from refs. 1, 2, 3, respectively. (**d**) One S model from ref. 4. Notice the remarkable consistency between all models on the outlined subduction-related features.

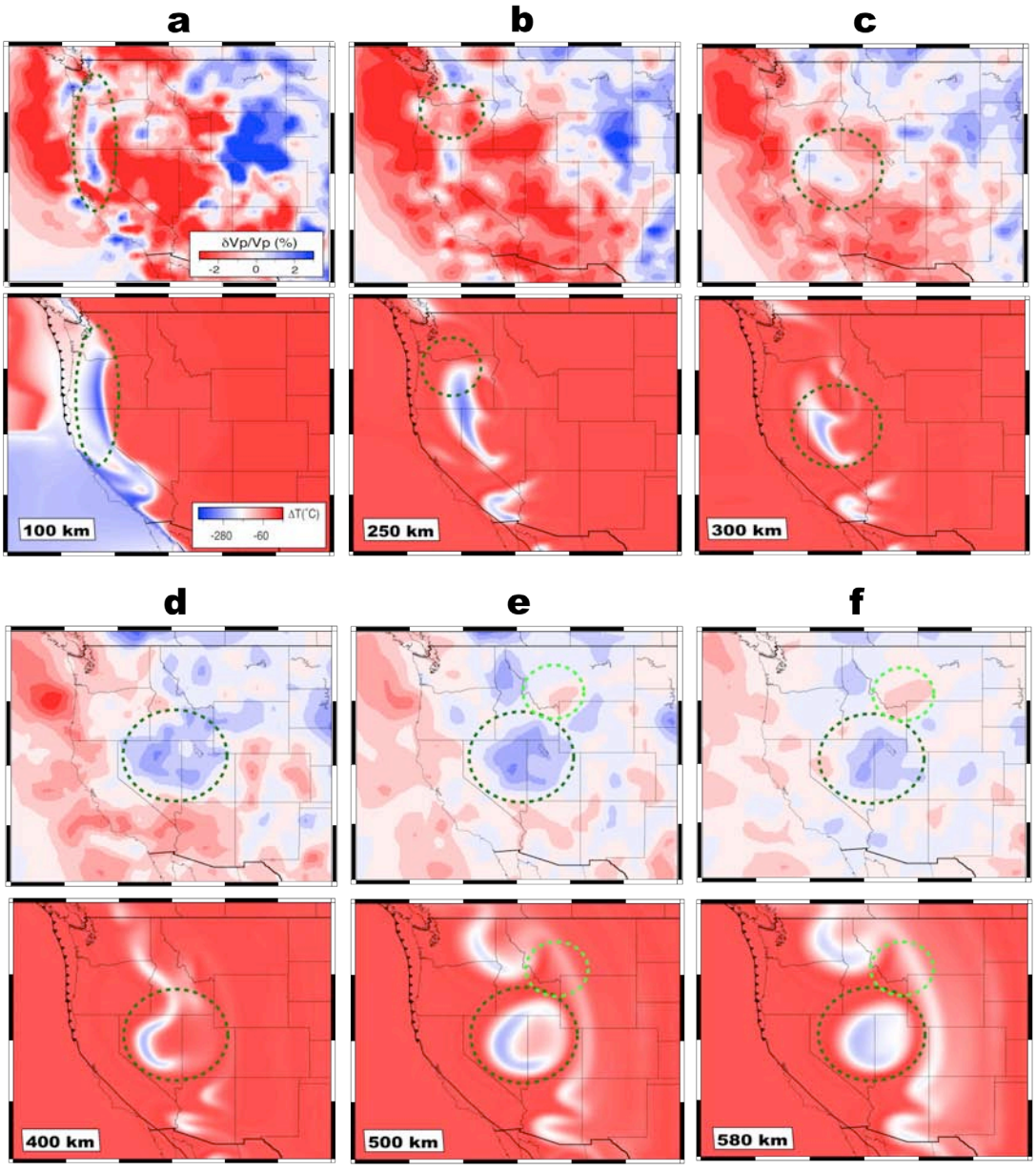

Figure S2. Comparison between observed[3] and predicted[5] upper mantle structure beneath western US at the same depth slices as shown in S1. The good match of the fast seismic anomaly at 300-600 km depths below Nevada and Utah suggests that this feature represents a segmented Farallon slab.

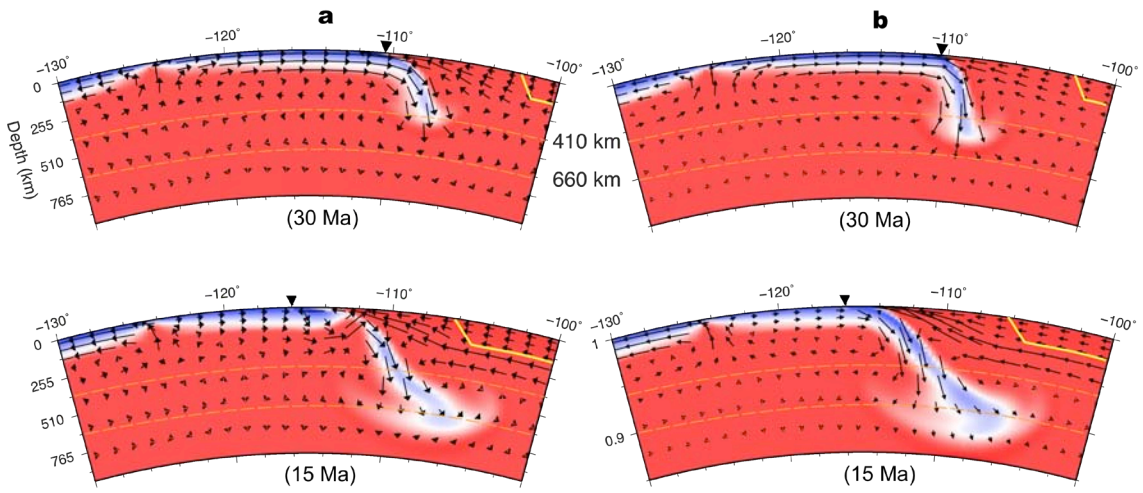

Figure S3. Effects of the 'sticky-air' layer on slab morphology. (**a**) Best-fit model with the 'sticky-air' function. (**b**) Same as case **a,** but with the 'sticky-air' layer removed. All sections are shown for 41°N, at two snapshots (30, 15Ma). Black triangles indicate trench position and the yellow outline is craton. Note the smaller slab dipping angles in case **a**, indicating a stronger sub-slab dynamic pressure. The slab-tear along the hinge occurring ~15 Ma in case **a** is absent in case **b**.

Reference

1. Burdick, S., *et al*., 2008, Model Update December 2008: Upper Mantle Heterogeneity beneath North America from P-wave Travel Time Tomography with Global and USArray Transportable Array Data, Seism. Res. Lett., 80, doi: 10.1785/gssrl.80.4.638.

2. Schmandt, B., and E. Humphreys, 2010, Complex subduction and small-scale convection revealed by body-wave tomography of the western United States upper mantle, Earth Planet. Sci. Lett., doi:10.1016/j.epsl.2010.06.047.

3. Sigloch, K., 2011, Mantle provinces under North America from multifrequency P wave tomography, Geochem. Geophy. Geosys., **12**, Q02W08, doi:10.1029/2010GC003421.

4. Tian, Y., Y. Zhou, K. Sigloch, G. Nolet, G. Laske, 2011, Structure of North American mantle constrained by simultaneous inversion of multiple-frequency SH, SS, and Love waves, J. Geophy. Res., **116**, B02307, doi:10.1029/2010JB007704.

5. Liu, L. & Stegman, D.R. Segmentation of the Farallon slab, Earth Planet. Sci. Lett., doi:10.1016/j.epsl.2011.09.027, **311**, 1-10.